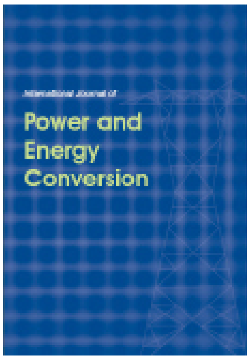

International Journal of Power and Energy Conversion

ISSN online: 1757-1162 - ISSN print: 1757-1154
https://www.inderscience.com/ijpec

Optimisation of FLUKA's cyclotron model for safety assessments: accuracy and uncertainty analysis in neutron ambient dose equivalent H*(10)

Ammar Bouabidi, Imen Hammami, Leila Ounalli

DOI: 10.1504/IJPEC.2025.10072505

Article History:

Received:	30 December 2024
Last revised:	01 June 2025
Accepted:	01 June 2025
Published online:	29 July 2025

Optimisation of FLUKA's cyclotron model for safety assessments: accuracy and uncertainty analysis in neutron ambient dose equivalent H*(10)

Ammar Bouabidi

Faculty of Sciences of Tunis,
University of Tunis El Manar,
2092, Tunisia
and
Research Laboratory on Energy and Matter for
Nuclear Science Development (LR16CNSTN02),
Ministry of Higher Education and Research, Tunisia
Email: ammar.bouabidi@gmail.com

Imen Hammami*

Research Laboratory on Energy and Matter for
Nuclear Science Development (LR16CNSTN02),
Ministry of Higher Education and Research, Tunisia
Email: imenhammemi99@gmail.com
*Corresponding author

Leila Ounalli

Research Laboratory on Energy and Matter for
Nuclear Science Development (LR16CNSTN02),
Ministry of Higher Education and Research, Tunisia
and
National Center for Nuclear Sciences and Technology,
Technopark Sidi Thabet, 2020 Ariana, Tunisia
Email: leila.ounalli@gmail.com

Abstract: A Monte Carlo model using the FLUKA code was developed to streamline dosimetry studies for proton cyclotrons, specifically for the IBA Cyclone®18. The model simulates two liquid targets – Large Volume Silver and Nirta®Conical8 niobium – allowing precise neutron fluence calculations in the vault room. The accuracy of the neutron ambient dose equivalent, H*(10), was validated using experimental data, with results showing strong agreement. The uncertainty analysis indicated a statistical error of less than 10% for neutron dose equivalent and 0.1% for neutron fluence. This model provides a reliable tool for optimising cyclotron installation safety, offering accurate neutron dosimetry with minimal statistical errors.

Keywords: FLUKA; cyclotron; target; niobium; silver; neutron ambient dose equivalent; accuracy; uncertainty.

Reference to this paper should be made as follows: Bouabidi, A., Hammami, I. and Ounalli, L. (2025) 'Optimisation of FLUKA's cyclotron model for safety assessments: accuracy and uncertainty analysis in neutron ambient dose equivalent H*(10)', *Int. J. Power and Energy Conversion*, Vol. 16, No. 6, pp.1–17.

Biographical notes: Ammar Bouabidi is currently pursuing a PhD in Nuclear Physics through a joint program between the Faculty of Science of Tunis (FST) and the Tunisian Center for Nuclear Sciences and Technology (CNSTN). He earned his Bachelor's in Fundamental Physics from FST and Master's in Quantum Physics. Then, he completed his Master of Science in Nuclear Power Plant Engineering at KEPCO International Nuclear Graduate School (KINGS) in South Korea. Through this academic journey, he has built strong expertise in reactor systems, radiation physics, and quantum theory, combining theoretical knowledge with applied nuclear engineering.

Imen Hammami specialises in medical imaging, and biomedical signal processing. Her research focuses on using Monte Carlo simulations and on integrating artificial intelligence into advanced imaging technologies to improve the diagnosis and treatment of various diseases. By bridging medical imaging with cutting-edge AI techniques, she aims to advance healthcare and enhance patient outcomes. He holds a PhD in Biophysics, Medical Physics, and Medical Imaging, along with a Master's and Bachelor's degree in related fields from the Higher Institute of Medical Technologies of Tunis. She also teaches at the institute.

Leila Ounalli has a Master's in Quantum Physics and PhD in Nuclear Physics, both obtained from Neuchâtel University. She started her career, concentrating on nuclear safety and medical applications. She manages radiation dosimetry initiatives with the IAEA and has specialised in radiation protection in Lausanne. She obtained research supervision accreditation from El Manar University. She pursued Advanced Studies in Medical Physics at ETH Zurich. She combines teaching and research in the field of medical physics. She is interested in radiation therapy, imaging, and radiation safety, aiming for a career in health physics.

1 Introduction

Four major manufacturers provide various cyclotron models and energy levels (https://nucleus.iaea.org/sites/accelerators/Pages/Cyclotron.aspx) [e.g., GE (Minitrace, PETtrace 09 – 16.5 MeV) (https://www.gehealthcare.com), IBA (Cyclone) (https://www.iba-radiopharmasolutions.com/cyclotrons), ACSI (TR19, TR24) (http://www.advancedcyclotron.com/cyclotron-solutions/tr19), (Eclipse 11 MeV)]. These medical cyclotrons produce radioisotopes, particularly the widely utilised radiopharmaceutical Fluoro-Deoxy-Glucose (FDG) in PET imaging (OCDE/AEN, 2005). During Fluorine production, protons interact with an enriched oxygen target. The neutron flux resulting from the $^{18}O(p, n)^{18}F$ reaction can escape from the cyclotron. It may be released into the cyclotron's components, such as the magnet coils (Bonvin et al., 2021), the bunkers (Vichi et al., 2020) and the atmosphere (Infantino et al., 2015a). In this context, Vichi et al. (2020) assessed the activation in PET cyclotron bunkers using Monte Carlo simulations. They implemented models of a GE PETtrace and an IBA Cyclone.

These models included their respective bunkers within the FLUKA code to identify the primary long-lived radionuclides generated. However, Bovin et al. (2021) determined the activation in cyclotron magnet coils by combining Monte Carlo calculation with RAW and ActiWIZ software's. In both studies, the discrepancies between calculated and measured activity values were attributed to the unknown actual composition of the materials assessed. In our developed FLUKA input code based on this limitation, we included the exact composition of each material in the cyclotron's geometry. These were done to ensure coherent results.

The Fluorine production process can lead to significant air activation and result in many contaminants. These contaminants primarily originate from nuclear reactions involving nuclei present in the air. Such reactions include neutron capture with the elemental constituents of air ($^{14}N(n, p)C^{14}$; $^{16}O(n, p)O^{17}$; $^{17}O(n, p)O^{18}$), including noble gases ($^{40}Ar(n, p)Ar^{41}$) (Infantino et al., 2015b). Upon release, these airborne contaminants, mainly ^{14}C and ^{41}Ar, emit beta and gamma radiation. This poses a radiation exposure risk to individuals nearby, especially cyclotron operators. The extent of air activation depends on some factors such as the neutron spectrum and the geometry of the cyclotron's infrastructure. Different PET centres typically share similar infrastructure and specific characteristics that can be generalised. Therefore, it would be more useful to have a standard model of cyclotron. This model can be adapted to the infrastructure of each site.

Providing a 'ready-to-use' input file that is, in fact, quite practical. To effectively assess the biological effects of neutron radiation on human tissue, it is essential to quantify the equivalent dose at specific points within a radiation field (Pelliccioni, 2000). The determination of this radiological protection operational quantity, expressed as neutron ambient dose equivalent H*(10) constitutes the main objective of this study. In addition, when constructing a new cyclotron site or adding a bunker to an existing facility, license holders often face the challenge of choosing the most appropriate technology for safety and production efficiency. Experimental studies, though available, can be expensive and time-consuming. Therefore, Monte Carlo simulations are a valuable tool for supporting safety assessments related to medical cyclotrons (Albiniak and Wrzesień, 2020). Although various codes are available, such as FLUKA (Battistoni et al., 2007; Battistoni et al., 2015; Böhlen et al., 2014; http://www.fluka.org/fluka.php), MCNP (Briesmeister, 1986), MCNPX (Benavente et al., 2015), MCNP6 (Alloni and Prata, 2017) and GEANT4 (Agostinelli et al., 2003). Not all of them are equally suitable for safety assessments related to low-energy medical cyclotrons. FLUKA, for instance, offers detailed models for low-energy neutron interactions, making it a strong candidate for these evaluations. MCNP, on the other hand, is highly versatile but may require extensive customisation for specific low-energy applications. GEANT4 is excellent for particle tracking. But, it may not be optimised for neutron transport at low energies, making it less efficient for these assessments. These differences underscore the importance of selecting the right code based on the specific requirements of the safety assessment. FLUKA is a well-validated Monte Carlo code, renowned for its effectiveness in modelling complex radiation environments and predicting radiation doses accurately. This is essential for safety assessments in medical and industrial applications. This makes FLUKA a valuable tool for radiation protection and safety studies. However, the accuracy of FLUKA predictions relies significantly on the precision of the optimised input parameters, including geometric design, materials, and physics approximations.

These predictions may be difficult to achieve through experimental or cost-effective methods. Any inaccuracies in these inputs can lead to significant errors in the simulations. While the comprehensive FLUKA manual provides detailed methods and tool descriptions (cards) in a general manner, it does not offer specific examples as found in the GEANT4 Monte Carlo code [Advanced Example STCyclotron (Albiniak and Wrzesień, 2020)]. Therefore, developing a general, robust, and detailed input is essential to conduct advanced simulations for tasks like radiation protection, safety report preparation, commissioning, and site modelling or modification for the same cyclotron facility rather than rebuilding from scratch (Briesmeister, 1986).

Over the past decade, many extensive studies have been conducted on the safety management and dosimetry of cyclotrons site through both experiments (Infantino et al., 2015a, 2016b; Albiniak and Wrzesień, 2020; Benavente et al., 2015) and Monte Carlo calculations using FLUKA (Infantino et al., 2015a, 2015b, 2016a; Infantino, 2015) and MCNP (Benavente et al., 2015; Alloni and Prata, 2017; Alloni et al., 2019). However, few studies have focused on determining accuracy and uncertainty and the relative error behaviour of detector positioning (Infantino et al., 2015a; Infantino, 2015). These studies focus solely on optimising the detector size to achieve minimal uncertainty while decreasing the FLUKA input run time. In this context, Infantino et al. (2015a) optimised the physical and transport parameters to estimate the accurate ambient dose equivalent H*(10) in four positions in the vault room around the TR19 PET cyclotron. An average ratio of 0.99 ± 0.07 between experimental measurements and simulations has been obtained. However, the four measurement positions were around the degrader and activation of the aquifer only.

This study also explores the relationship between the accuracy and uncertainty of the detector's positions, simulation time, and CPU cost. Our proposed approach addresses the challenge in pure analogue simulations, where minimising uncertainty typically demands significant computational resources. To our knowledge, the accuracy and uncertainty of the neutron ambient dose equivalent H*(10) around medical cyclotrons, along with the detailed design of the entire target, have not been previously studied using FLUKA or other Monte Carlo codes. This work provides a more precise understanding of overall radiation safety. It also enhances the visibility and impact of scientific research.

2 Materials and methods

2.1 Overview of IBA cyclotron geometry

The IBA Cyclone® 18 is renowned for delivering beam energies of 18 MeV for protons and 9 MeV for deuterons. It operates with high beam currents, achieving 100 μA for protons and 40 μA for deuterons. Its versatility is demonstrated by a dual extraction system with eight ports, accommodating various applications (https://www.iba-radiopharmasolutions.com/cyclotrons). The cyclotron accelerates protons within a 1.35 Tesla magnetic field. It weighs 25 tons with dimensions of 2 metres in diameter and 2.2 metres in height. It features a deep valley magnet made of low-carbon iron (electromagnetic steel) and four legs constructed from stainless steel. The technical design of the bunker with Portland concrete density of 2.35 g/cm^3 within a 4 m × 6 m vault room (Riga et al., 2018; El Azzaoui et al., 2023). The bunker's wall is designed for ease of construction and on-site decommissioning (International Atomic Energy Agency, 2009).

2.2 Study strategy

In this study, we focused on three cyclotron models: PETtrace (GE) (https://www.gehealthcare.com), TR19 (ACSI) (http://www.advancedcyclotron.com/cyclotron-solutions/tr19), and Cyclone18 (IBA) (Table 1) (https://www.iba-radiopharmasolutions.com/cyclotrons). All three are designed to produce Fluorine-18 by directing a proton beam at a liquid target containing enriched water $H_2{}^{18}O$ (97%). The detailed geometry of the IBA medical cyclotron has been developed to assess the neutron ambient dose equivalent H*(10). This model includes an experimentally substantiated and optimised detector for measuring the ambient equivalent dose H*(10). The IBA developed model simulates a cyclotron generating protons with an energy of 18 MeV. However, the PETtrace (GE) and the TR19 (ACSI) were chosen for their similarities to the IBA cyclone®18 model to assess neutron fluence. Notably, the PETtrace cyclotron incorporates a silver insert material related to that of the IBA cyclotron. It is used to evaluate the total neutron fluency outside the target. Conversely, the TR19 cyclotron is utilised to investigate the neutron energy fluence within the target solution. It leverages its unique target insert materials. In addition, the analysis of the uncertainty and the accuracy for analogue FLUKA computing was performed.

2.3 FLUKA setup

The FLUKA Monte Carlo code (version 2021.2.2) was employed to integrate the geometry of IBACyclone®18 cyclotron model (Ferrari et al., 2005). Implemented in FORTRAN, FLUKA Monte Carlo code installed on a high-performance Linux system with specific hardware requirements (8Go of RAM, CPU 3.00 GHz, 64 bits and Core i5). The code involved a meticulous process for defining geometric complexities, specifying beam characteristics, and detailing material properties. Such a comprehensive approach guarantees an accurate representation of the cyclotron model (Figure 1). Additionally, to simplify the creation and edition of FLUKA input file, the FLAIR user-friendly graphical interface version 2.3-0 was used (Vlachoudis, 2009).

The simulation input omits the internal structure of the IBA cyclotron and the associated beamline components used in proton therapy. It concentrates instead on the target design for FDG production (Słonina et al., 2014).

Two liquid targets are included: the large volume 'LV' target with a silver insert and the Conical8 target with a niobium insert (Table 1).

The left part of Figure 2 provides detailed views of the LV silver insert. In Figure 2(e), the LV target comprises four distinct areas, including the front silver insert filled with 2 cm^3 of enriched water ($H_2{}^{18}O$) 97%, shown in lime green. The target body, illustrated in green, along with the cooling water diffuser, is made of brass. The cooling water, represented in blue, circulates beneath both the brass and silver inserts, playing an essential role in maintaining optimal operating conditions. This design integrates seamlessly with the broader framework of the IBACyclone®18 cyclotron, offering a comprehensive understanding of its functionality and applications in radioisotope production. Similarly, the right side of Figure 2 presents meticulously designed 3D and plan cross-sectional views of the Conical8 niobium insert target. Figure 2(f) illustrates the various components of the target designed in FLUKA. Positioned at the end of the collimator, the front of the target features a conical area with a niobium insert depicted in purple, 1 mm thick and wider at the bottom (Alloni et al., 2019). The inner conical area was filled with 2.27 cm^3 of enriched water ($H_2{}^{18}O$) 97%, highlighted in lime green, representing the target solution, as described in Table 2. The outer body of the target coloured in red, constructed from black anodised aluminium, contributes to the target's structural integrity. Cooling water shown in blue circulates between the cone insert and the target body, which is important for maintaining optimal operating conditions.

Table 1 Composed materials used to model cyclotron facility

Material	*Composition*	*Density (g/cm^3)*
Concrete (1)	Carbon (23%), silicon (12%), hydrogen (10%), oxygen (40%), calcium (12%), magnesium (2%)	2.34
Concrete (2)	Hydrogen (1%), oxygen (52.91%), magnesium (0.2%), silicon (33.70%), calcium (4.4%), carbon (0.1%), sodium (1.6%), aluminium (3.38%), potassium (1.3%), iron (1.4%)	2.3
Stainless-steel	Chromium (18%), iron (74%), nickel (8%)	8
ICRUmat	Oxygen (76.2%), hydrogen (10.1%), carbon (11.1%), nitrogen (2.6%)	1
O_18	-	0.001429
Water_18	O_18 (1%) Hydrogen (2%)	1.1
TarSol	Water (3%) Water_18 (97%)	1.1

Figure 1 Cyclotron design and shielded bunker, (a) technical drawing (b) FLUKA schematic

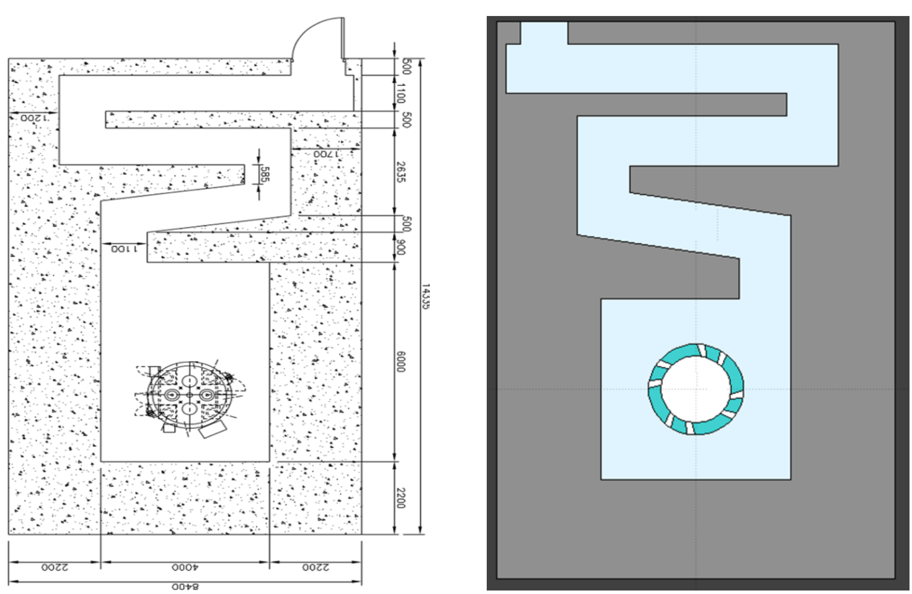

(a) (b)

Figure 2 Targets, (a) the back of the LV silver insert (b) the Conical8 niobium target (c) 3D view of the LV silver target in Flair (d) 3D view of the conical target in Flair, (e, f) plan cuts of the LV silver and Conical8 targets in Flair (see online version for colours)

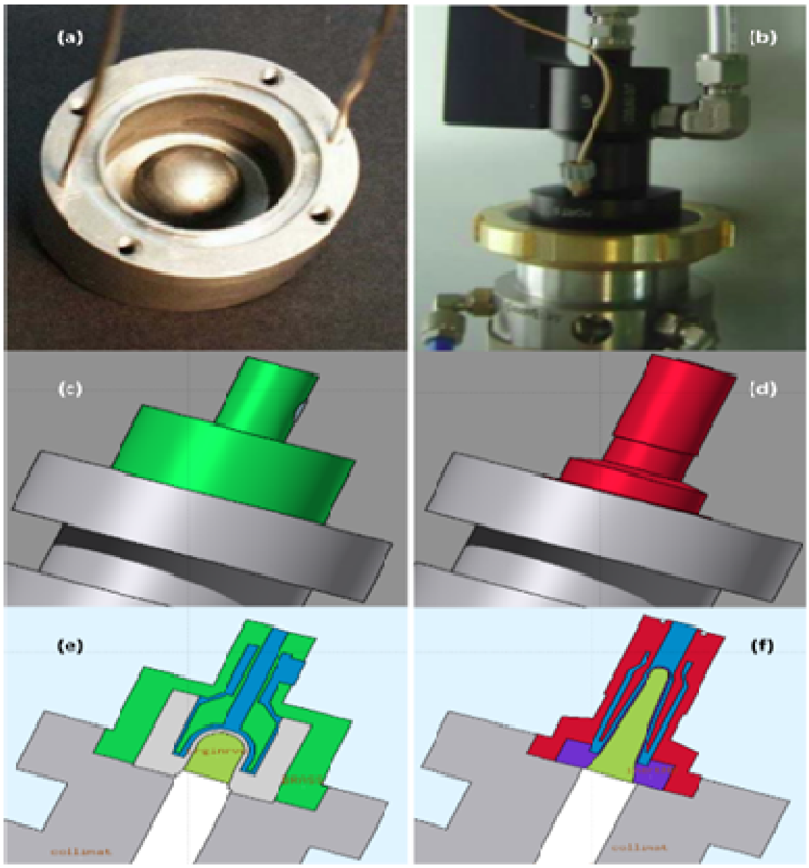

2.4 *Input structure description*

The developed input for simulation contains six main parts: beam, geometry, materials, physics, transport and scoring. The beam and BEAMPOS cards were used to define the proton beam characteristics. A Gaussian distribution of proton beam is predominantly utilised with a maximum energy of 18 MeV and intensity of 100 μA along the horizontal direction of the acceleration (z-axis) with the width in the x direction measured at 0.216 cm (FWHM), and the width in the y direction at 0.301 cm (Tamburella and Giles, 2008). The geometry part includes cards that detailed the cyclotron facility compositions divided into various regions assigned to the corresponding material (Table 1). To perform our experiment two targets conical and cylindrical were modelled as described in Section 2.3. Physics card specifies the physics models and particle transport settings. COALESCE and EVAPORAT physics cards were used for the activation of coalescence mechanism and the evaporation of heavy fragments respectively. The scoring cards are customised to measure specific quantities such as fluence distribution, neutron ambient equivalent dose H*(10), fluencies of proton, neutron and photon. The neutron ambient equivalent dose was estimated utilising the USRBIN card (X-Y-Z Cartesian and region scoring) with the AUXSCORE card allowing the association between the estimator and the conversion factors (Table 2). In addition, the USRTRACK card was used to estimate the fluence distribution for neutron, photon, and proton particles. Three transport cards were involved in our simulations which are: RADDECAY used to simulate the radioactive decays, IRRPROFI used to establish an irradiation profile for calculations related to radioactive decay, and DCYTIMES which specifies decay times for the evaluation of radioactive product yields.

Table 2 Scoring and transport cards

Metrics	*Scoring cards*	*Transport cards*	*Supplement cards*
Fluence (proton, neutron and photon)	USRTRACK (linear)	None	None
Fluence distribution	USRBIN (Cartesian)	None	None
Ambient dose equivalent H*(10) (neutron and photon)	USRBIN (region)	None	AUXSCORE

Figure 3 Detectors positioning around the IBA Cyclone®18 (see online version for colours)

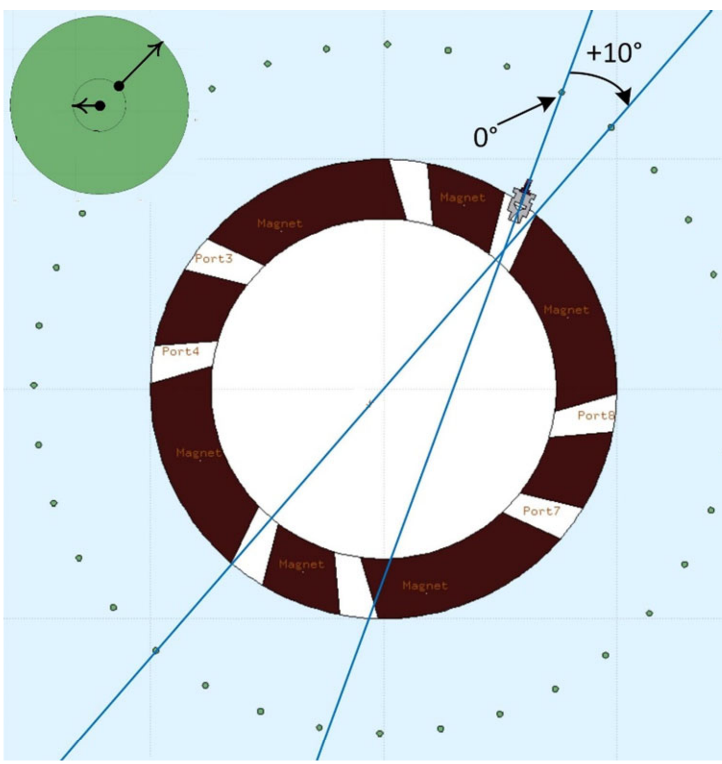

Following the guidelines outlined in ICRU Report 43 (ICRU, n.d.), the original ICRU sphere was utilised as a reference to estimate the neutron ambient equivalent dose H*(10). This sphere represents tissue with a diameter equivalent to 30 cm, where the ambient dose is measured at a depth (d) of 10 mm for the whole body. However, in this study to estimate the neutron ambient equivalent dose in the IBA cyclotron facility, we modelled the detector as a sphere that contains another sphere (Figure 3). The inner sphere was designated as a scoring region, and the radius of the detector volume was optimised with an agreement to experimental data (Alloni and Prata, 2017). To optimise the detector radius, 36 detectors, designed following ICRU recommendations and filled with ICRUmat material as outlined in Table 1, were utilised. The detectors were positioned 50 cm from the outer surface of the cyclotron along the middle plane and the beam axis, with placements made at every 10° intervals. The detector positioned at the proton beam axis was designated as the 0° position, while the azimuth angle varied according to the compass direction from which the proton beam originated. The central position geometry of the detector is illustrated in Figure 3.

2.5 Uncertainty assessment

Effectively handling uncertainty, accuracy, and CPU cost is pivotal in simulation strategy to yield reliable results that align with experimental data. The accuracy of the simulation largely hinges on the detector design and material selection, which are closely intertwined with experimental data. Striking a balance to achieve the lowest CPU cost without compromising accuracy is a key consideration in this study. A targeted uncertainty level below 10% was deemed satisfactory as is customary in Monte Carlo simulation for achieving convergence (Marco, 2016). However, attaining the ultimate accuracy for the ambient equivalent dose H*(10) necessitates running multiple iterations to fine-tune the detector size. The initial phases of this benchmark study were executed on a standard computer with performance as mentioned in Section 2.3. Subsequently, upon completion of the design and time estimation phases, an Amazon Elastic Compute Could (EC2) with 16 cores and 32 GB RAM was employed to improve computational efficiency, coping with the growing simulation complexity. This optimisation strategy ensures a prudent equilibrium between achieving accurate results and efficiently managing computational resources.

3 Results and discussion

3.1 Input testing

In order to evaluate the developed input, first USRBIN cards in Cartesian scoring (X-Y-Z) were employed to estimate the proton flux in both LV and Conical8 targets (Figure 4). This estimation aims to verify the precise targeting of the proton beam onto the solution at the designated position. This step ensures alignment accuracy and safeguards against misalignments that could impact the simulation results later. The proton beam, represented in striking black and red hues, was effectively simulated using the FLUKA code, as illustrated in Figure 4.

In the second step of input testing, the simulation entails evaluating the neutron yield spectrum and comparing the outcomes with those from other cyclotrons, notably TR19 (ACSI) and PETtrace (GE). The trends in neutron fluence both inside and outside the LV target are analysed for the IBA Cyclone®18, and their consistency with other cyclotrons is observed (Figure 5). The results affirm that the FLUKA model yields reliable assessments of neutron fluence comparing to data from (Infantino, 2015).

Figure 4 Proton beam alignment, (a) the LV silver target (b) the Conical8 niobium target (see online version for colours)

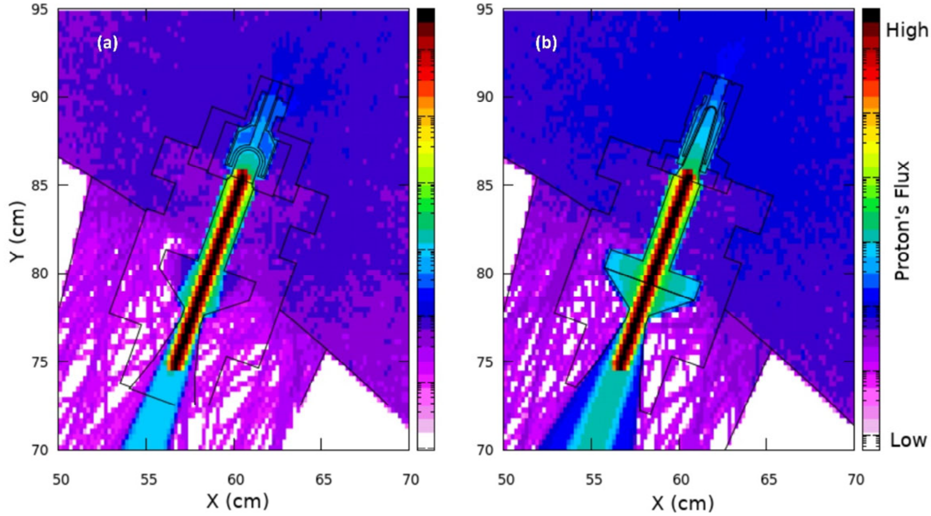

Figure 5 Neutron fluence, (a) in the target: the IBACyclone®18(blue) and the ACSI TR19 cyclotron (red) (b) in the vault room: the IBACyclone®18 (blue) and the PETtrace cyclotron (red)

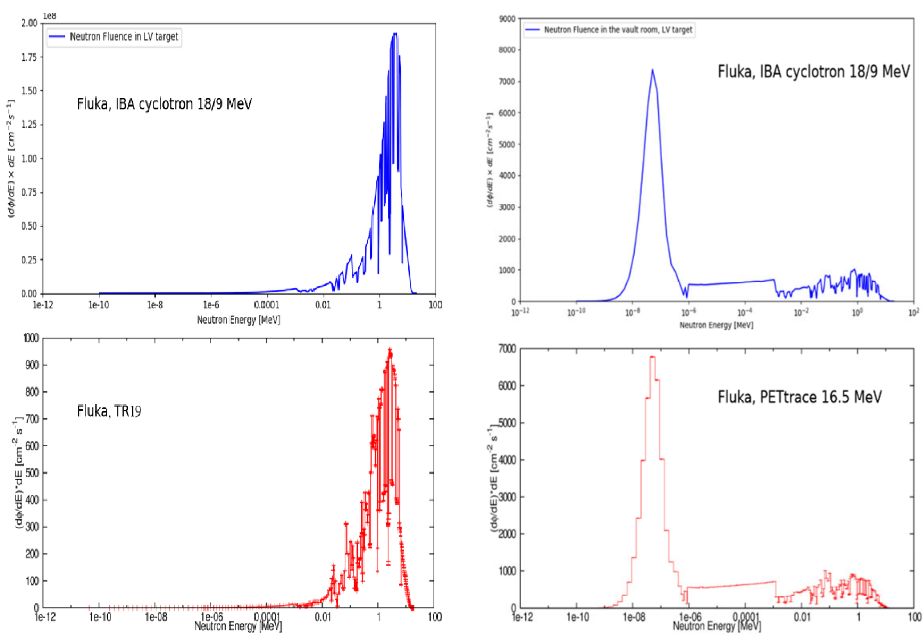

(a) (b)

Source: Infantino (2015)

3.2 Neutron ambient equivalent dose using large volume target

3.2.1 Optimisation of detector volume

Once the FLUKA input is verified, we have opted to estimate the neutron equivalent dose H*(10). The simulation was conducted under the same conditions as experiments carried out at the cyclotron 18/9 MeV with the LV silver target at the Flucis facility (IBA). The neutron dose was estimated at 36 positions within the cyclotron vault room using an adapted ICRU sphere introduced in Section 2.3. The modified ICRU sphere volume undergoes validation via FLUKA simulations and experimental measurements (Alloni and Prata, 2017), by assessing various detector radii (R_0 = 0.35 cm, R_1 = 0.40 cm, R_2 = 0.42 cm, R_3 = 0.45 cm, R_4 = 0.50 cm). The analysis revealed that a detector radius of R_2 = 0.42 cm is optimal for the neutron ambient equivalent dose calculations (Figure 6). A good agreement between neutron ambient equivalent dose H*(10) obtained using FLUKA with the adjusted ICRU sphere and experimental measurements with a mean difference values of less than 10%.

Figure 6 Optimisation of detector radii for the neutron ambient equivalent dose calculation (see online version for colours)

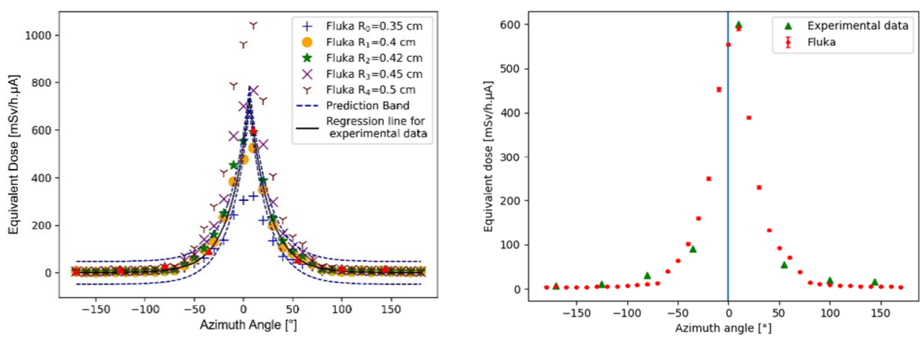

(a) (b)

The adjusted ICRU sphere is deemed verified for calculating neutron ambient equivalent dose H*(10) at any position within the cyclotron vault room. Since, the developed input has been verified and tested as described above, it can now be used with the Conical8 target.

3.2.2 Neutron ambient equivalent dose using Conical8 target

Now the detector volume is optimised, it is applied to estimate the neutron ambient equivalent dose H*(10) with the Conical8 target. Therefore, a thorough comparison between the LV silver target and Conical8 niobium target is conducted, considering angular neutron ambient equivalent dose H*(10) in the vault room. The marginal increase in neutron fluence in the cyclotron vault, as depicted in Figure 7, translates into variations in H*(10). Specifically, the detector at 10° received an additional 100 mSv/h.µA from the Conical8 target compared to the LV target. Moreover, the detector at 0° still experienced an additional 50 mSv/h.µA from the LV target. This phenomenon is attributed to the fluctuations in neutron fluence distribution across energy and space. The target solution volumes in LV and Conical8 are 2 ml and 2.27 ml, respectively. Notably, the Conical8 target possesses a larger volume of enriched water, potentially leading to a higher occurrence of $^{18}O(p, n)^{18}F$ reactions.

Figure 7 Assessment of neutron ambient equivalent dose around the cyclotron for LV and Conical8 targets (see online version for colours)

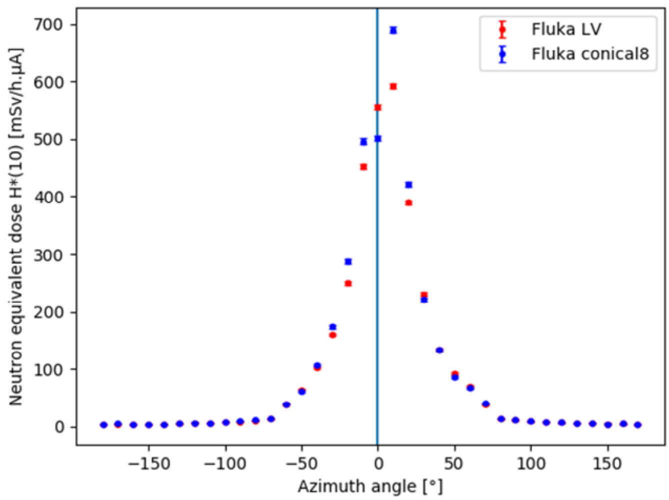

Figure 8 Comparison of neutron fluence in LV and conical8 targets: (a) The neutron fluence in the target solution, (b) The neutron fluence in the vault room

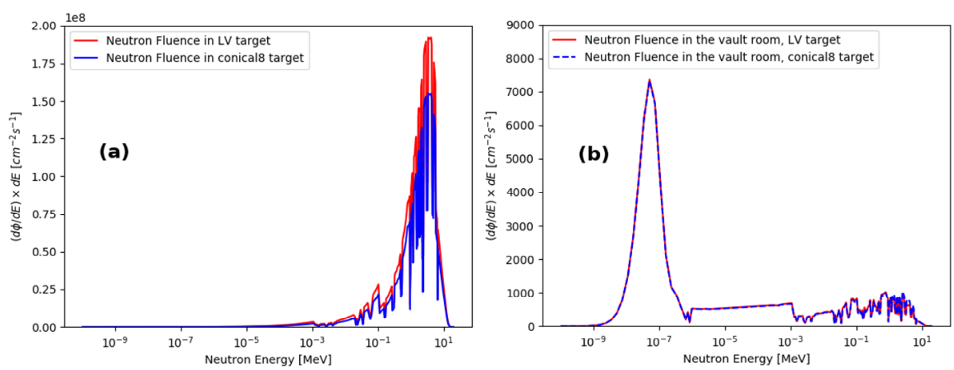

3.3 *Neutron fluence distribution*

The neutron fluence distribution was compared for the LV silver target and Conical8 in two distinct manners: in the target solution [Figure 8(a)], and in the vault room [Figure 8(b)]. The results reveal variations in neutron fluence distribution due to disparities in target volumes and reaction probabilities. This disparity arises from the fact that the cross-sectional area of the conically shaped niobium inserts diminishes from the interior to the exterior. Consequently, certain proton beams have a lower probability of interaction within the filled volume of the target. For thermal neutrons, the total neutron fluence for two targets remains similar [Figure 8(b)]. Nonetheless, a slight difference is apparent around 1 MeV. The fluence of the Conical8 target slightly exceeds that of the LV target. This variation in total fluence inside and outside the target is attributed to the attenuation factors of the two targets. As noted in various studies (Infantino et al., 2015a, 2015b, 2016a, 201b; Infantino, 2015), the trends and peak flux exhibit a decrease.

3.4 Evaluation of uncertainty

The uncertainty in the simulation is influenced by the position and volume of the detector as shown in Figure 9. Greater distance from the signal source necessitates more computational power and time to achieve the same level of uncertainty. Changes in detector volume led to decreased accuracy, underscoring the importance of experimental verification to establish the credibility of simulations. The uncertainty in the estimation of neutron ambient equivalent dose H*(10) depends on the detector volume, the number of simulated primaries, and the distance from the target. Larger detector volumes require fewer primaries to achieve the same level of uncertainty, thus reducing simulation time. Regarding neutron ambient dose equivalent [Figures 9(a) and 9(b)] for LV and Conical8 targets respectively, the relative error of all H*(10) estimation around the cyclotron remains below 10%. The distribution exhibits a convex pattern, with the lowest value observed in the 10° detector. The proximity of the detector to the target corresponds to a decrease in the relative error.

Figure 9 The angular distribution of relative error percentage for H*(10) estimation in detectors for: (a) the LV target, (b) the Conical8 target (see online version for colours)

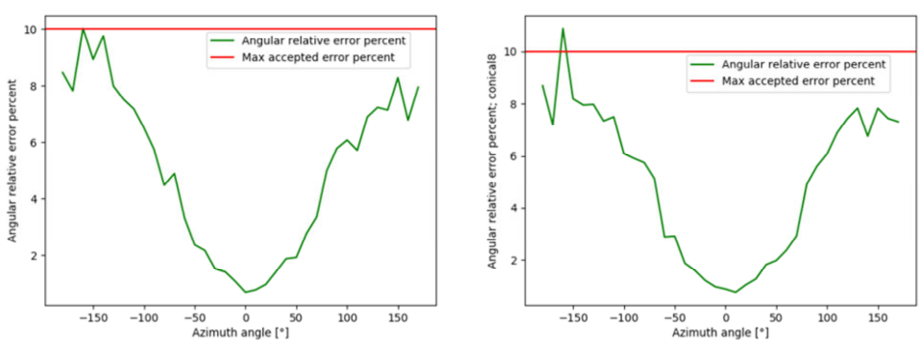

(a) (b)

The conducted simulation for 2 days and 15 hours, demonstrates relative errors below 0.1% for neutron fluence [Figure 10(b)] and less than 10% for neutron ambient dose equivalent [Figures 9(a) and 9(b)] around the cyclotron. As illustrated in Figure 10(b), for neutron energies above 0.01 eV (10^{-8} MeV), the relative error of the total neutron fluence remains below 0.1% within the two-target solutions: LV and Conical8 targets. At the boundary of the neutron energy region below 0.01 eV and near 20 MeV, the uncertainty peaks [Figures 10(c) and 10(d)], while between these two points, the uncertainty diminishes to less than 0.1%. This delineates a specific range where a given total neutron fluence is considered reliable and accurate.

Figure 10 The relative error percentage in both targets: (a) and (c) the fluencies inside and outside the LV target; (b) and (d) The fluencies inside and outside the Conical8 (see online version for colours)

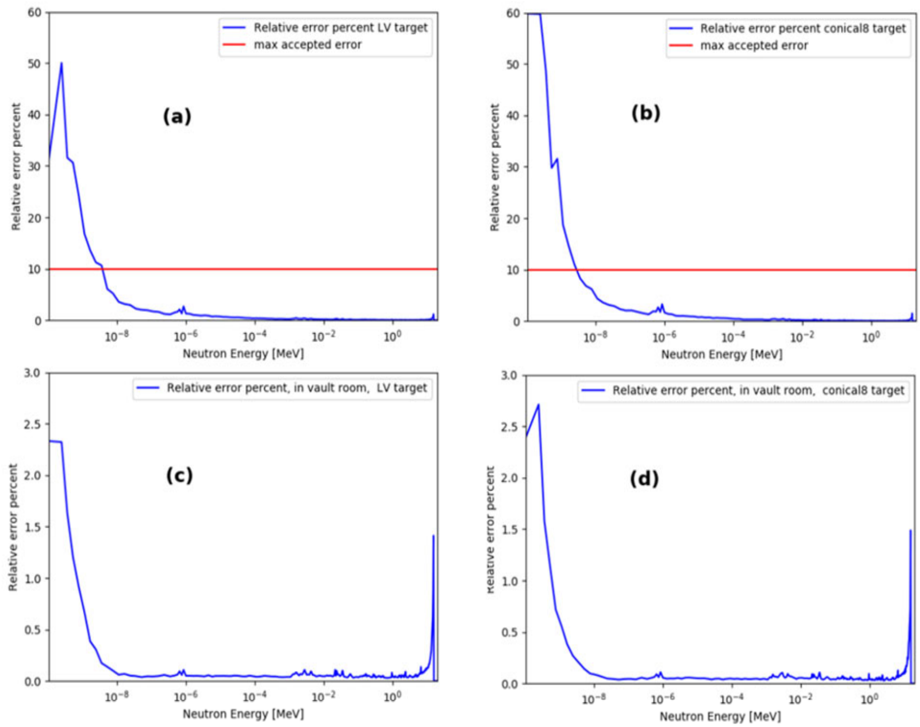

3.5 Limitation

The main constraint in Monte Carlo simulations is runtime, requiring substantial computational resources to minimise runtime and produce results with decreased uncertainty. This input highlights that detectors situated further from the radiation source demand longer runtime or additional CPU resources for parallel simulations to attain acceptable uncertainty levels. It underscores that as the distance from the radiation source expands, so does the uncertainty, emphasising the need for careful consideration and allocation of computational resources for efficient simulations.

4 Conclusions and future perspective

A comprehensive design of the IBA Cyclone®18 cyclotron was carefully developed in FLUKA Monte Carlo and subjected to thorough verification and testing processes. This input is an accurate and precise tool for dosimetry studies, particularly for computing neutron fluence in both liquid targets for Fluorine-18 production and the cyclotron air volume, including the vault room. Additionally, it calculates the neutron ambient dose equivalent H*(10) in the vault room, with uncertainty dependent on detector location.

The developed input includes a reliable detector model based on the ICRU sphere, capable of measuring neutron ambient dose equivalent H*(10) several positions in the vault room. Uncertainties related to detector positions were assessed, along with an evaluation of the computing detrimental effects of radiation required to maintain them within acceptable limits. Achieving greater precision requires additional computational time or CPUs. Future investigations will explore biasing techniques in FLUKA to reduce simulation time, enhance dosimetry measurement aspects, and improve radiation protection in proton cyclotrons.

Acknowledgements

We would like to show our gratitude to Mr. J.M. Geets, for sharing information and technical specifications of the Cyclone®18 cyclotron, the LV silver target and Nirta®Conical8 niobium target design with us during this research. Our gratitude to Pr. J-L. Vuilleumier for reviewing this paper and to FLUKA experts (Dr. P. Sala and Dr. A. Infantino) for their precious comments.

This work was supported by the IAEA Coordinated Research Project JO2014 [Contract: 26426].

References

Advanced Cyclotron Systems, Inc., *TR-19 Cyclotrons*, ACSI – Advanced Cyclotron Systems Inc. [online] http://www.advancedcyclotron.com/cyclotron-solutions/tr19 (accessed 24 June 2022).

Agostinelli, S. et al. (2003) 'GEANT4 – a simulation toolkit', *Nucl. Instrum. Methods Phys. Res. A: Accel. Spectrom. Detect. Assoc. Equip.*, Vol. 506, No. 3, pp.250–303, https://doi.org/10.1016/S0168-9002(03)01368-8.

Albiniak, Ł. and Wrzesień, M. (2020) 'Using Monte Carlo methods for Hp (0.07) values assessment during the handling of 18F-FDG', *Radiat. Environ. Biophys.*, Vol. 59, No. 4, pp.643–650, https://doi.org/10.1007/s00411-020-00864-9.

Alloni, D. and Prata, M. (2017) 'Characterisation of the secondary neutron field generated by a compact PET cyclotron with MCNP6 and experimental measurements', *Appl. Radiat. Isot.*, Vol. 128, pp.204–209, https://doi.org/10.1016/j.apradiso.2017.07.031.

Alloni, D., Prata, M. and Smilgys, B. (2019) 'Experimental and Monte Carlo characterization of radionuclidic impurities originated from proton irradiation of [18O] H2O in a modern medical cyclotron', *Appl. Radiat. Isot.*, Vol. 146, pp.84–89, https://doi.org/10.1016/j.apradiso.2019.01.026.

Battistoni, G. et al. (2015) 'Overview of the FLUKA code', *Ann. Nucl. Energy*, Vol. 82, pp.10–18, https://doi.org/10.1016/j.anucene.2014.11.007.

Battistoni, G., Cerutti, F., Fasso, A., Ferrari, A., Muraro, S., Ranft, J., Roesle, S. and Sala, P.R. (2007) 'The FLUKA code: description and benchmarking', *AIP Conference Proceedings*, AIP, Batavia, Illinois (USA), pp.31–49, https://doi.org/10.1063/1.2720455.

Benavente, J.A. et al. (2015) 'Neutron spectra due 13N production in a PET cyclotron', *Appl. Radiat. Isot.*, Vol. 99, pp.20–24, https://doi.org/10.1016/j.apradiso.2015.01.029.

Böhlen, T. et al. (2014) 'The FLUKA code: developments and challenges for high energy and medical applications', *Nucl. Data Sheets*, Vol. 120, pp.211–214, https://doi.org/10.1016/j.nds.2014.07.049.

Bonvin, V., Bochud, F., Damet, J., Theis, C., Vincke, H. and Geyer, R. (2021) 'Detailed study of the distribution of activation inside the magnet coils of a compact PET cyclotron', *Appl. Radiat. Isot.*, Vol. 168, https://doi.org/10.1016/j.apradiso.2020.109446.

Briesmeister, J.F. (1986) *MCNP: A General Monte Carlo Code for Neutron and Photon Transport*, Version 3A, Revision 2, USA [online] https://www.osti.gov/biblio/5191995-mcnp-general-monte-carlo-code-neutron-photon-transport-version-revision (accessed 3 June 2024).

Cyclone 18/9. Site Requirements Guide [online] https://www.iba-radiopharmasolutions.com/cyclotrons (accessed 10 June 2024).

El Azzaoui, B., Messous, MY., Didi, A., Chakir, E.M. and Alibrahmi, E.M. (2023) 'Evaluation of radiation protection properties of novel concrete mixture against photon energy in nuclear applications: simulation and experimental findings', *International Journal of Power and Energy Conversion (IJPEC)*, Vol. 14, No. 4, pp.376–392.

Ferrari, A., Paola, R.S., Fasso, A. and Ranft, J. (2005) *FLUKA: A Multi-Particle Transport Code*. Report Number CERN-2005-010, SLAC-R-773, CERN.

FLUKA-Team, *The Official FLUKA Site* [online] http://www.fluka.org/fluka.php (accessed 3 June 2024).

General Electric Company, *PETtrace 800 Cyclotron Series* [online] https://www.gehealthcare.com (accessed 10 June 2024).

Infantino, A. (2015) *Advanced Aspects of Radiation Protection in the Use of Particle Accelerators in the Medical Field*, PhD thesis, University of Bologna [online] https://core.ac.uk/download/pdf/76519795.pdf (accessed 24 June 2023).

Infantino, A. et al. (2016a) 'Assessment of the neutron dose field around a biomedical cyclotron: FLUKA simulation and experimental measurements', *Phys. Med.*, Vol. 32, No. 12, pp.1602–1608, https://doi.org/10.1016/j.ejmp.2016.11.115.

Infantino, A., Marengo, M., Baschetti, S., Cicoria, G., Vaschetto, V.L., Lucconi, G., Massucci, P., Vichi, S., Zagni, F. and Mostacci, D. (2015a) 'Accurate Monte Carlo modeling of cyclotrons for optimization of shielding and activation calculations in the biomedical field', *Radiat. Phys. Chem.*, Vol. 116, pp.231–236, https://doi.org/10.1016/j.radphyschem.2015.01.001.

Infantino, A., Oehlke, E., Mostacci, D., Schaffer, P., Trinczek, M. and Hoehr, C. (2016b) 'Assessment of the production of medical isotopes using the Monte Carlo code FLUKA: simulations against experimental measurements', *Nucl. Instrum. Methods Phys. Res. Sect. B Beam Interact. Matter. At.*, Vol. 366, pp.117–123, https://doi.org/10.1016/j.nimb.2015.10.067.

Infantino, A., Valtieri, L., Cicoria, G., Pancaldi, D., Mostacci, D. and Marengo, M. (2015b) 'Experimental measurement and Monte Carlo assessment of Argon-41 production in a PET cyclotron facility', *Phys. Medica*, Vol. 31, No. 8, pp.991–996, https://doi.org/10.1016/j.ejmp.2015.07.146.

International Atomic Energy Agency (2009) *Cyclotron Produced Radionuclides: Guidelines for Setting up a Facility*, Technical Reports Series No. 471 [online] https://www.iaea.org/publications/8046/cyclotron-produced-radionuclides-guidelines-for-setting-up-a-facility (accessed 24 June 2022).

International Atomic Energy Agency, *Database of Cyclotrons for Radionuclide Production* [online] https://nucleus.iaea.org/sites/accelerators/Pages/Cyclotron.aspx (accessed 3 June 2024).

International Commission on Radiation Units and Measurements (ICRU), *Determination of Dose Equivalents from External Radiation Sources – Part II*, Report 43 [online] https://www.icru.org/report/determination-of-dose-equivalents-from-external-radiation-sources-part-ii-report-43/ (accessed 24 June 2022).

Marco, D.Z. (2016) *Methodology for Data Validation 1.0 (Handbook)*, Essnet Validate Foundation, Publications Office of the European Union in Luxembourg.

OCDE/AEN (2005) *Beneficial Uses and Production of Isotopes: 2004 Update, Nuclear Development*, OECD Publishing, Paris, https://doi.org/10.1787/9789264008823-en.

Pelliccioni, M. (2000) 'Protection quantities and conversion coefficients for use in radiation shielding', *Journal of Nuclear Science and Technology*, Vol. 37, No. 1, pp.850–854, https://doi.org/10.1080/00223131.2000.10875010.

Riga, S., Cicoria, G., Pancaldi, D., Zagni, F., Vichi, S., Dassenno, M., Mora, L., Lodi, F., Morigi, M.P. and Marengo, M. (2018) 'Production of Ga-68 with a General Electric PETtrace cyclotron by liquid target', *Phys. Med.*, Vol. 55, pp.116–126, https://doi.org/10.1016/j.ejmp.2018.10.018.

Słonina, D. et al. (2014) 'Relative biological effectiveness of the 60-MeV therapeutic proton beam at the Institute of Nuclear Physics (IFJ PAN) in Kraków, Poland', *Radiat. Environ. Biophys.*, Vol. 53, pp.745–754, https://doi.org/10.1007/s00411-014-0559-0.

Tamburella, C. and Giles, T.J. (2008) 'Beam diagnostics for an 18MeV medical cyclotron', *Nucl. Instrum. Methods Phys. Res. Sect. B Beam Interact. Mater. At.*, Vol. 266, pp.4678–4681, https://doi.org/10.1016/j.nimb.2008.05.115.

Vichi, S. et al. (2020) 'Activation studies for the decommissioning of PET cyclotron bunkers by means of Monte Carlo simulations', *Radiat. Phys. Chem.*, Vol. 174, https://doi.org/10.1016/j.radphyschem.2020.108966.

Vlachoudis, V. (2009) 'Flair: a powerful but user friendly graphical interface for FLUKA', *International Conference on Mathematics, Computational Methods & Reactor Physics*, Saratoga Springs, New York.